INFECTION AND IMMUNITY, Oct. 1992, p. 4154–4167
0019-9567/92/104154-14$02.00/0

Vol. 60, No. 10

Experimental Verocytotoxemia in Rabbits

SUSAN E. RICHARDSON,[1,2]* TAMARA A. ROTMAN,[1,2] VENITA JAY,[3] CHARLES R. SMITH,[3] LAURENCE E. BECKER,[3] MARTIN PETRIC,[1,2] NANCY F. OLIVIERI,[4] AND MOHAMED A. KARMALI[1,2]

Departments of Microbiology,[1] Pathology,[3] and Paediatrics,[4] The Research Institute of The Hospital for Sick Children, Toronto, Ontario M5G 1X8, and Department of Microbiology, University of Toronto, Toronto, Ontario M5S 1A1,[2] Canada

Received 28 February 1992/Accepted 23 July 1992

The clinicopathologic effects of intravenously administered purified verocytotoxin 1 (VT1; Shiga-like toxin 1) in 2-kg male rabbits was studied. The 50% lethal dose was 0.2 μg of protein per kg of body weight (2×10^4 50% cytotoxic doses per kg). The clinical features included nonbloody diarrhea and a progressive flaccid paresis, usually culminating in death. The histopathology was characterized by edema and hemorrhage in the mucosa and submucosa of the cecum and edema, hemorrhage, and neuronal necrosis in the brain and gray matter of the spinal cord. Thrombotic microangiopathy, the characteristic histopathologic renal lesion in the hemolytic-uremic syndrome, was also found to be the underlying lesion in verocytotoxemic rabbits. To determine the specific distribution of VT1 in rabbit tissues, purified ^{125}I-labelled VT1 was administered intravenously to 20 rabbits (both immunologically naive and VT1-immune rabbits). The highest specific uptake of ^{125}I-VT1 was in the spinal cord, brain, cecum, colon, and small bowel in unimmunized animals but in the liver, spleen, and lungs in immune animals. Immunofluorescent staining of cecal and spinal cord tissues after intravenous administration of VT1 showed evidence of specific vascular endothelial cell binding of the toxin. The striking correlation of the central nervous system and gastrointestinal localization of ^{125}I-VT1 with the sites of known histopathology is consistent with direct toxin-mediated injury to these tissues, initiated by the specific binding of VT1 to the vascular endothelium. We conclude that the vascular damage induced by VT1 in affected rabbit tissues is similar to that seen in the kidneys and other tissues in patients with verocytotoxin-producing *Escherichia coli*-associated hemolytic-uremic syndrome. This suggests that although the rabbit model fails to replicate human hemolytic-uremic syndrome, it is useful for studying the pathogenesis of the vascular lesions in verocytotoxin-producing *E. coli*-associated diseases.

The classical hemolytic-uremic syndrome (HUS) consists of a triad of clinical features (acute renal failure, thrombocytopenia, and microangiopathic hemolytic anemia) that follows a bloody diarrheal illness (9). Pathologically, HUS is characterized by microvascular angiopathy that affects not only the kidneys but a variety of other tissues and organs, including the gastrointestinal (GI) tract, central nervous system (CNS), lungs, heart, and pancreas (9). The endothelial cell damage observed in damaged vessels has led to the hypothesis that endothelial cells are the primary target sites for the inciting agent(s) of HUS (6, 14).

In 1985, work from our laboratory demonstrated a close association between classical HUS and infection by verocytotoxin (VT)-producing *Escherichia coli* (VTEC) (15). We reported that patients with HUS develop enteric infection with VTEC, that free VT is present in fecal filtrates, and that patients with VTEC infection develop rising antibody titers to VT (15). This led us to postulate that VT is directly responsible for the genesis of HUS and is probably the factor that causes primary damage to endothelial cells in affected vessels (14).

The term VT refers to a group of closely related subunit toxins named VT1, VT2, VT2v, and VTe (10, 28). Since the prototype toxin, VT1, is virtually identical to Shiga toxin (from *Shigella dysenteriae* type 1) (31), VTs are also referred to as Shiga-like toxins (21). All members of this toxin family have the same polypeptide structure, enzymatic activity, and ability to bind to specific glycolipid receptors that possess the terminal disaccharide galactose-α-1,4-galactose in their carbohydrate moiety (14). VT1 and Shiga toxin have molecular weights of about 70,000 and consist of an A subunit and five copies of a B subunit (14, 21). In vitro studies have demonstrated that the holotoxin binds via the B subunit to the glycolipid globotriaosyl ceramide (Gb3) in the cell membrane (18) and is internalized by the process of receptor-mediated endocytosis (26a). VT1, the first of these *E. coli* cytotoxins to be characterized, has been shown to exhibit cytotoxicity to a restricted number of cultured cell lines, including Vero, HeLa (21), and human endothelial (22) cells. VT1 is lethal to mice after parenteral challenge (21) and causes fluid secretion in rabbit ileal loops (21) and diarrhea in infant rabbits after oral challenge (23).

Our hypothesis implicating VT as the factor that causes primary vascular endothelial cell damage assumes that the toxin passes intact into the circulation from the bowel after enteric infection by VTEC and then interacts specifically with endothelial cells in target tissues. To test the hypothesis that circulating VT causes microvascular damage, we investigated the effects of systemic VT1 administration in rabbits. In this report we provide evidence that the histopathological changes observed are the result of vascular damage associated with specific binding of VT1 to endothelial cells in this experimental model.

MATERIALS AND METHODS

Toxin purification. VT1 was purified by using a scheme of differential ammonium sulfate precipitation and sequential chromatography on hydroxylapatite, chromatofocusing, and

* Corresponding author.

Cibachron blue columns as described previously (24). VT1 was obtained from two sources during the course of these experiments: (i) *E. coli* H30 (O26:K60:H11) (16) (J. Konowalchuk, Health Protection Branch, Health and Welfare Canada, Ottawa, Canada) and (ii) JB28, an *E. coli* TB1 strain transformed by recombinant plasmid pUC18 containing the VT1 genes cloned from bacteriophage H19B (13) (J. Brunton, Toronto, Ontario, Canada). The VT1 obtained from JB28 was extracted from a 3-liter culture containing 50 μg of carbenicillin per ml and grown for 24 h at 37°C. The extraction procedure differed from that previously described (24) only in that the cell extract obtained by incubation with polymyxin B was concentrated by Amicon filtration on a YM10 membrane and the retentate was dialyzed against a 0.01 M phosphate buffer at pH 7.2. The toxin purified from either source revealed two bands (32 and <10 kDa) on tricine-sodium dodecyl sulfate-polyacrylamide gel electrophoresis (27), consistent with the A and B subunits of purified VT (24). Both preparations produced toxin; after dilution for injection into the rabbits, the toxin tested negative in the *Limulus* amebocyte lysate assay (E-toxate; Sigma) at a detection level of 0.05 to 0.1 endotoxin unit/ml.

The biological activity of the VT was monitored by cytotoxicity on Vero cells as previously described to determine the 50% cytotoxic dose (CD_{50}) (15). One CD_{50} is defined as the amount of VT activity required to produce a 50% cytopathic effect in a Vero cell monolayer after 3 days of incubation at 37°C. The methods described above produced VT1 with a biological activity of approximately 10^5 to 10^6 CD_{50}/μg of protein.

Radiolabelling of VT1. Purified toxin was equilibrated by dialysis with 0.05 M sodium borate buffer (pH 8.5) and then concentrated through a Centricon-10 concentrator with a molecular weight cutoff of 10,000 (Amicon Corp.). The toxin from either source was reacted with the Bolton and Hunter reagent containing 1 mCi of ^{125}I (ICN Biomedicals, Montreal, Canada) as recommended by the manufacturer. The preparation was then chromatographed through a Bio-Gel P-100 column (1.6-cm diameter, 80 cm long) in phosphate-buffered saline (PBS), and the eluate was monitored for radioactivity and biological activity. Toxin from the pooled fractions (8- to 12-ml total volume) with the highest levels of cytotoxicity had specific activities of 2×10^5 to 5×10^5 cpm/μg of protein with biological activities of 10^4 to 10^6 CD_{50}/μg of protein. The radioactive protein recovered after the iodination had minimal loss in biological activity. The initial preparation contained a total of 6×10^6 CD_{50}, whereas the final preparation contained a total of 2×10^6 CD_{50}. On analysis by reducing 12% polyacrylamide gel electrophoresis and autoradiography, both preparations contained only two bands, one of 32 kDa and one of <10 kDa.

Radiolabelling of BSA. Two hundred micrograms of bovine serum albumin (BSA) was radiolabelled in the same manner as VT1 and then chromatographed through a Bio-Gel P-100 column to remove free iodine. A pooled preparation of fractions with high levels of radioactivity had 1.9×10^6 cpm/μg. This preparation contained a single band of 60 kDa on analysis by polyacrylamide gel electrophoresis and autoradiography.

Clinicopathologic studies with VT1-challenged rabbits. The 50% lethal dose (LD_{50}) was determined in 24 New Zealand White rabbits (Reimens Fur Ranches) weighing 2 kg each. Each rabbit was challenged intravenously with 1 ml of a solution of purified VT1 per 2 kg via the marginal ear vein. Three rabbits were challenged at each of eight doses, decreasing by threefold dilutions from 4×10^4 to 19 CD_{50}/kg (0.4 to 1.9×10^{-4} μg/kg) to determine the LD_{50}. The LD_{50} and 50% symptomatic dose results were calculated by the method of Reed and Muench (25).

TABLE 1. Dosage range in rabbits

Dose (CD_{50}/kg)	No. of rabbits	No. of LD_{50}s/kg
3.2×10^3	1	0.16
4×10^3	4	0.2
4.5×10^3	3	0.22
8×10^3	2	0.4
1.3×10^4	3	0.65
2×10^4	2	1.0
3.2×10^4	3	1.5
4×10^4	4	2.0
1×10^5	8	5.0

Nine rabbits from the LD_{50} group given the three highest doses of VT1 were combined with 21 additional rabbits to make a working group of 30 test animals on which subsequent descriptive studies were based. Seven control animals were challenged with injections of sterile saline. The dosage range of the two groups combined is shown in Table 1.

Rabbits were observed for the clinical effects of toxin until death or sacrifice. Diarrhea was defined as unformed stool that adhered in sticky clumps to the cage floor or the perineum or was grossly watery or bloody. Every 24 h, urine samples from selected rabbits were collected by using a metabolic cage designed to funnel the urine into a collecting bottle. Wire mesh was added to the bottom of the metabolic cages to prevent stool from contaminating the urine collection. The urine samples were quantitated and then subjected to dipstick urinalysis with Labstix (Ames, Miles Laboratories, Etobicoke, Ontario, Canada). Microscopic analysis was not attempted because there were large amounts of crystals in the urine (a normal finding in rabbits).

Occult blood testing on stool was done with Hematest tablets (Ames). The following biochemical and hematologic variables were examined in selected rabbits: measurement of sodium, chloride, urea, and creatinine in serum; hemoglobin concentration; leukocyte count; platelet count; and reticulocyte count. The erythrocyte morphology was assessed on blood films prepared and stained (Wright stain) in the hematology department and read by a hematologist (N.F.O.), who was blinded to the treatment status of the animals.

Rabbits were sacrificed by intravenous injection of pentobarbital at approximately 0.5 ml/kg (Euthanyl, 240 mg/ml; MTC Pharmaceuticals, Cambridge, Ontario, Canada). Samples of representative organs were obtained, fixed, and processed. The brain was removed from the bony skeleton at the time of death and immediately fixed in Formalin. For fixation of the spinal cord, the entire vertebral column was removed after the ribs were disarticulated. The dorsal spinous process and underlying dura mater were then removed over several vertebral levels to expose the spinal cord. The entire bony column was then immersed in Formalin for at least 24 h; the spinal cord was then removed for routine histology.

Intravenous administration of ^{125}I-VT1 to rabbits. VT1 was administered to immune and nonimmune rabbits. Four rabbits were immunized with VT1. The first three doses were administered subcutaneously as a toxoid solution of 50 μg of VT1 treated with glutaraldehyde (4). The first dose was administered in complete Freund's adjuvant, and two subsequent doses were administered in incomplete adjuvant.

Three more doses of active holotoxin were administered intravenously without adjuvant at a dose equivalent to the LD_{50} (0.2 μg/kg). The neutralizing antibody titers on Vero cell monolayers became positive after the second immunization and reached peaks of 1:1,024 to 1:4,096.

Twenty rabbits were injected through the marginal ear vein with doses ranging from 1×10^6 to 5.5×10^6 cpm of toxin. To determine the half-life of VT in the blood, 1-ml aliquots of blood were sampled from the artery of the ear at defined intervals after injection in 15 (11 immunologically naive, 4 immune to VT1) of the 20 rabbits. The half-life of ^{125}I-BSA (2×10^6 cpm) was determined in the same manner in one other rabbit. The total amount of labelled toxin or BSA present in the blood was quantitated by monitoring for radioactivity on a Beckman gamma counter and multiplying the radioactivity per milliliter by the estimated total blood volume (55 ml/kg of body weight) (17). All rabbits were sacrificed 1 or 2 h after intravenous challenge for the localization studies ($n = 14$) and at 0.03, 2, 9, and 24 h for a time course study ($n = 8$).

After pentobarbital sacrifice of the animals, individual organs were removed, weighed, and then analyzed for radioactivity. Samples of tissues weighing approximately 1 to 4 g (heart, lungs, liver, spleen, kidneys, stomach, jejunum, ileum, cecum, colon, skeletal muscle, brain, and spinal cord) were counted for radioactivity. GI contents and the intestinal wall were analyzed separately at all levels of the GI tract. The radioactivities of the blood and urine were also quantitated.

Histopathology. Specimens were taken from the heart, lungs, liver, spleen, pancreas, stomach, small intestine, cecum, colon, kidneys, skeletal muscle, brain, and spinal cord. Rabbit tissues were preserved in 10% buffered formaldehyde immediately after removal. They were embedded in paraffin and sectioned at 8 to 10 μm for all organs except the kidney, which was sectioned at 4 μm. All sections were stained with hematoxylin and eosin plus specific fibrin stains where indicated (phosphotungstic acid-hematoxylin, picromallory stain, Lendrum-Morris stain). The histopathologic analysis was performed by one observer blinded to the treatment status of the animals.

Twelve of the 30 VT-treated rabbits that had GI symptoms and lacked encephalitozoan disease (29) were chosen for detailed histopathology of the GI tract. Of the four GI control rabbits, one had to be eliminated from the analysis because of the presence of encephalitozoan disease in the CNS. Five of the 30 VT-treated rabbits were selected for detailed histopathologic analysis of the CNS. These rabbits, which were sacrificed during the acute stage of their disease, had neurologic signs and lacked encephalitozoan disease. Of the four CNS controls, one was removed from the analysis because of encephalitozoonosis.

Histopathological classifications were done as follows. (i) For the GI tract, cecal sections were assessed in each of four categories (mucosal edema, mucosal hemorrhage, submucosal edema, and submucosal hemorrhage) on a scale of 0 to 3+, representing absent, mild, moderate, and severe pathology, respectively. A minimum of 50 blood vessels per section were observed, and the number of abnormal vessels per 50 vessels was determined. (ii) For the CNS, three brain sections (anterior [cerebral hemispheres, including frontal areas and basal ganglia], middle [cerebral hemispheres, including temporoparietal areas, thalamus, and basal ganglia], and posterior [cerebellum and brainstem]) and three spinal cord sections (cervical, thoracic, and lumbar) were assessed for each animal. The sections were graded in each of four categories (edema, hemorrhage, thrombosis, and infarction) on a scale of 0 to 3+.

Immunofluorescence detection of VT1. Two male New Zealand White rabbits weighing 2 kg were challenged intravenously, one with a 3-mg bolus of purified VT1 (test) and one with 2.5 ml of PBS (control). Two hours later, under anesthesia and after heparinization, the blood was purged from the body by concomitant infusion of intravenous saline and bleeding from the femoral artery, until the withdrawal was clear and about 700 ml of saline had been infused. Cecal and spinal cord sections were taken and immediately frozen in optimal cutting temperature compound (Tissue-Tek; Miles) in plastic cryomolds in liquid nitrogen and stored at −70°C until sectioning. Sections were cut at 6 μm, and adjacent sections were stained with hematoxylin and eosin and an immunofluorescent stain. For the immunofluorescence studies, the slides were brought to room temperature, fixed in paraformaldehyde, dehydrated in ethanol gradients, and incubated with a 1:200 (cecal) or 1:100 (spinal cord) dilution of mouse anti-VT1 monoclonal antibody PH1 (1) (C. Lingwood, Toronto, Ontario, Canada) for 20 min at room temperature. After three washes in PBS, the slides were incubated with a 1:10 dilution of affinity-purified goat anti-mouse immunoglobulin G-F(ab')$_2$-fluorescein isothiocyanate antibody (Cappel-Organon Teknika Inc.) preadsorbed with normal rabbit serum overnight at 5°C. The slides were rinsed three times in PBS, stained with 0.01% Evans blue solution, and rinsed once more with PBS; coverslips with glycerol and *p*-phenylenediamine were added. The slides were examined and photographed under a Reichert-Jung fluorescence photomicroscope.

Statistics. Standard errors of the means were determined for all values shown in the figures. The Student *t* test was used to determine significance.

RESULTS

Clinical features. The LD_{50}, as determined in 24 immunologically naive rabbits given purified intravenous VT1, was 0.2 μg of VT1 per kg of body weight (2×10^4 CD_{50}/kg). The 50% symptomatic dose was 1.8×10^3 CD_{50}/kg. The group of 30 rabbits analyzed, which included 9 of the rabbits in the LD_{50} group (see Materials and Methods), received a mean dose of 3.9×10^4 CD_{50}/kg. The mean time to death of rabbits that died or were sacrificed in a moribund state was 1.9 days (range, 0.5 to 3 days) ($n = 14$) (mean dose, 4.2×10^4 CD_{50}/kg; median dose, 3.2×10^4 CD_{50}/kg). The mean time to sacrifice in the rest of the rabbits ($n = 16$), which were either asymptomatic ($n = 3$) or mildly to moderately symptomatic ($n = 13$), was 4.1 days (range, 2 to 10 days) (mean dose, 3.7×10^4 CD_{50}/kg; median dose, 1.6×10^4 CD_{50}/kg). The asymptomatic rabbits received doses of VT that were 0.65× ($n = 1$) and 0.22× ($n = 2$) the LD_{50}. The controls ($n = 7$) were sacrificed at a mean of 8.6 days (range, 3 to 16 days). Affected rabbits appeared ill about 24 h postchallenge; clinical signs appeared as early as 18 h. The earliest signs of illness were general listlessness, ruffled fur, anorexia, and decreased water consumption, accompanied by a decreasing urine output and weight loss. There were only two symptomatic rabbits that survived for a week (dose, 10^5 CD_{50}/kg). They lost 17 and 23% of their respective body weights during the first week postchallenge; two healthy controls each gained 16% of their body weight over the same time.

In addition to systemic signs, gastrointestinal and neurological signs were prominent. Of the 30 rabbits given VT1, 15 (50%) developed diarrhea that varied from loose, sticky stool

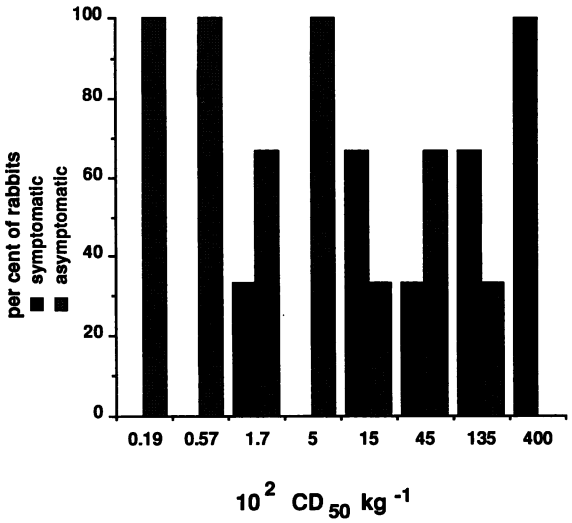

FIG. 1. Dose response in rabbits given intravenous VT1. The percentage of rabbits with symptoms (GI or CNS or both) increases at increasing doses of VT1 (expressed as 10^2 CD_{50}/kg). Data on three rabbits at each of eight doses are shown. The LD_{50} is 200 × 10^2 CD_{50}/kg.

(without blood or mucus) to severe watery diarrhea causing perianal staining, accompanied in three cases by gross blood and mucus. Occult blood was found in the stool in three cases of nonbloody diarrhea. The mean VT dose for rabbits with diarrhea was 4.1 × 10^4 CD_{50}/kg, whereas the mean dose of those without diarrhea was 3.8 × 10^4 CD_{50}/kg (not statistically significant). Onset of the diarrhea occurred at a mean of 1.6 days postchallenge and lasted an average of 7 days, at which time overall clinical improvement was evident. Thirteen of the 15 affected animals had mild to moderate diarrhea. Clinically severe GI involvement was manifested not only by severe diarrhea (n = 2; doses, 0.4× and 5.0× LD_{50}) but also by a syndrome consistent with paralytic ileus, manifested by abdominal distension and lack of stool (n = 1; dose, 0.65× LD_{50}).

Seventeen (57%) of the rabbits challenged with VT1 developed CNS symptoms. The mean dose of those with CNS symptoms was 4.7 × 10^4 CD_{50}/kg; for those without CNS symptoms, the mean dose was 3 × 10^4 CD_{50}/kg (not statistically significant). A minority (3 of 18 rabbits) died within the first 24 h without the appearance of focal neurologic signs. Clinically detectable signs were noted at a mean of 1.8 days after intravenous challenge. Involvement commonly began with asymmetric extremity paresis (forelimb paresis usually preceded hindlimb paresis). Four animals had transient paresis lasting 24 to 36 h, but in the majority of rabbits the paresis became progressively and rapidly more severe. Just before death, the muscles of the trunk, head, and neck were severely paralyzed, and the animal lay on its side with neck extended, exhibiting shallow, rapid respirations. Convulsions were not observed.

The presence or absence of symptoms (GI, CNS, or both) was found to correlate directly with the administered dose of VT1 (Fig. 1), although the mean time to death did not. Three rabbits that were transiently symptomatic after the initial intravenous VT challenge were subsequently immunized against VT1 by using active holotoxin intravenously. After a detectable neutralizing antibody titer to VT1 developed, the rabbits were entirely resistant (clinically and pathologically) to further intravenous VT challenge, even at doses of 10 to 100× the LD_{50}.

Laboratory results. (i) Urinalysis and renal function. After VT1 challenge in the test rabbits, there was a drop in urine output that was statistically significant for the second 24-h collection ($P < 0.05$) (Table 2). Hematuria, ketonuria, and glycosuria were not features of VT intoxication, and the pH of all specimens was alkaline at 8.0 to 8.5 (normal). However, proteinuria increased as the intoxication progressed, with significantly elevated levels from the collections at days 1 and 2 ($P < 0.05$) (Table 2). Measurements of renal function showed a transient elevation of creatinine in serum on day 1 ($P < 0.05$), followed by a rise in urea in serum on days 2 and 3 ($P < 0.01$) and a return to normal by one week postchallenge in survivors (Table 2).

(ii) Biochemistry and hematology. Modest rises in serum sodium and chloride occurred early after the administration of toxin, although they did not achieve statistical significance (Table 2). The hematology results showed no significant alterations in mean hemoglobin concentration, leukocyte count, and reticulocyte count on any day after VT challenge (Table 2). Blood films were examined from specimens taken before and at 1, 2, 3, and 8 days after VT1 challenge in five test rabbits and one control. There were no detectable changes from the baseline in the blood films after VT administration for any of the test animals or the control rabbit.

Pathology. (i) Gastrointestinal tract. At autopsy, the most obvious gross abnormality was mild to severe edema of the cecal mucosa, accompanied by mucosal petechiae and hemorrhages and by serosal petechial hemorrhages in the severe cases. The cecal contents were usually loose and watery and did not adhere to the mucosa as in normal rabbits. In two cases, grossly bloody stool was present. The associated mesentery was edematous in some cases, although visible edema of the small bowel, stomach, or colon was not evident.

Light microscopy of the cecum revealed characteristic changes in the mucosa and submucosa that were not present in control rabbits ($P < 0.01$) (Fig. 2a). Mucosal edema and hemorrhage, without ulceration, were prominent features in all but one VT-treated animal (Fig. 3). Mucosal hemorrhage varied from mild to severe and focal to diffuse and was not associated with acute (neutrophilic) inflammation. Scattered eosinophils were present in the mucosa, but there was no significant difference between test and control animals. Vascular abnormalities in the mucosa were prominent (Fig. 2a) and correlated with the severity of edema and hemorrhage in the gut wall. Small feeding blood vessels of the intercrypt mucosa, located in the lamina propria adjacent to the muscularis mucosa, were most commonly affected. The abnormalities ranged from vascular wall changes (loss of definition and smudging of the architecture of the wall; Fig. 4a, inset) to luminal occlusion by a finely reticular pink deposit in the lumen (Fig. 4a) to fibrinoid necrosis of the vessel wall (replacement of normal structure by a deposit of amorphous, pink, hyaline, fibrinlike material; Fig. 4b). A mean of 10 of 50 abnormal mucosal vessels was found (range, 5 to 20 of 50) in the cecal sections.

Submucosal abnormalities were similar to those seen in the mucosa, although the edema was much more striking and the hemorrhage was less severe. The occurrence of both edema and hemorrhage was statistically different from that of controls ($P < 0.01$) (Fig. 2a). Vascular thrombosis was present in the submucosal vessels of half of the rabbits examined. The serosa generally appeared normal, although

TABLE 2. Biochemical, hematologic, and clinical variables in rabbits treated with intravenous VT1[a]

Day(s)	Concn in serum				Hemoglobin concn (g/liter)	Blood cell counts (10^9/liter)			Urine vol (ml)	Protein concn in urine (mg/dl)
	Na (nmol/liter)	Cl (nmol/liter)	Creatinine (mol/liter)	Urea (nmol/liter)		Leukocytes	Platelets	Reticulocytes		
0	140.1 ± 2.0 (10)	100.3 ± 2.2 (10)	66.1 ± 0.9 (12)	4.5 ± 0.7 (12)	115 ± 9.7 (6)	12 ± 3.4 (6)	586 ± 168 (6)	0.06 ± 0.02 (4)	183 ± 65.5 (4)	16 ± 11.9 (8)
1	140.4 ± 1.4 (8)	100.5 ± 2.1 (8)	79.9 ± 13.4[b] (7)	4.1 ± 0.8 (8)	110.7 ± 5 (7)	10.6 ± 4 (7)	467 ± 149 (7)	0.06 ± 0.02 (5)	101 ± 47.7 (4)	30 ± 0[c] (3)
2	143.0 ± 4.4 (3)	105.3 ± 4.5 (3)	57.3 ± 22.8 (3)	5.6 ± 0.5[c] (3)	119 ± 8.6 (6)	9.3 ± 6 (6)	440 ± 175 (5)	0.04 ± 0.01 (5)	55 ± 34[b] (4)	65 ± 40.4[b] (4)
3	145.0 ± 7.5 (3)	104.0 ± 4.0 (3)	62.7 ± 19.5 (3)	7.4 ± 1.3[c] (3)	118 ± 6.4 (3)	14.4 ± 5 (3)	443 ± 185 (3)	0.07 ± 0.01 (3)	65 ± 50 (2)	
8	140.0 (1)	105.0 (1)	59.0 (1)	5.5 (1)	106 ± 13 (2)	13 ± 1.4 (2)	668 ± 439 (2)	0.04 ± 0.04 (2)		
8–16									162 ± 96.5 (7)	530 ± 980.9 (4)
16	138.5 ± 0.7 (2)	100.5 ± 0.7 (2)	53.5 ± 12.0 (2)	4.4 ± 0.1 (2)	100 ± 4.2 (2)	13 ± 4.3 (2)	329 (1)			

[a] All values are means ± standard errors; *n* values are given within parentheses.
[b] $P < 0.05$ versus corresponding control group.
[c] $P < 0.01$ versus corresponding control group.

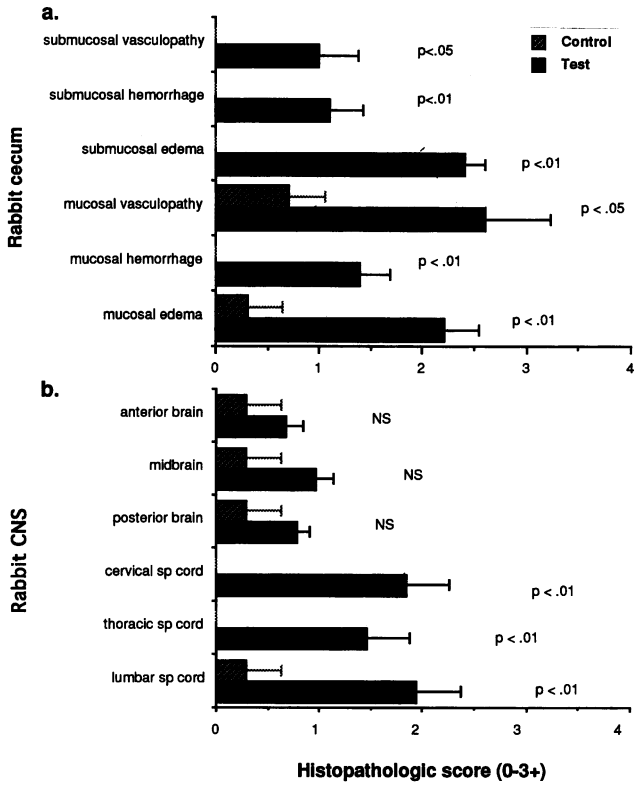

FIG. 2. Histopathological effects of intravenous VT1 in rabbit cecum and central nervous system. (a) Severity of VT1-induced pathology in the cecum: means of scores (0 to 3+) for each of six features (mucosal or submucosal hemorrhage, edema, and vasculopathy) in 12 test rabbits and 3 controls. (b) Brain and spinal cord abnormalities analyzed in a similar fashion in five test rabbits and three controls. Error bars represent the standard errors of the means.

two rabbits had a mild degree of serosal edema and hemorrhage without vascular abnormalities.

Sections of the stomach ($n = 4$), small intestine ($n = 6$), and colon ($n = 4$) in test rabbits with documented cecal pathology and in appropriate controls ($n = 5$) were examined. The histology of the stomach and small intestine was normal in all test and control rabbits. Colonic histopathology was normal in three of four test animals and in controls. One test rabbit had a moderate acute inflammatory infiltrate with a significant eosinophilic component in the colon, cecum, and small intestine in the absence of any VT-related changes. Minimal eosinophilic infiltrates were common in both control and test animals in small and large gut sections.

(ii) CNS. The gross appearance of the brain was normal in all rabbits. The spinal cord appeared tense and swollen within the dural sheath at the levels of the cervical and lumbar enlargements in some animals. Visible foci of hemorrhage were prominent in the grey matter at these levels in cross-sections of the cord.

The microscopic abnormalities in the spinal cord affected the grey matter most prominently (Fig. 5, inset), with occasional extension into the adjacent white matter. The mildest changes observed in the spinal cord were areas of focal grey matter hemorrhage, which were patchy, mild, and rarely associated with mild edema. More advanced lesions showed patches of vacuolation caused by edema of the

FIG. 3. Marked hemorrhage (a) and edema in the mucosa and submucosa of the rabbit cecum after intravenous VT1. The epithelium is intact, and no inflammation is present. Dilated lymphatics are present (b). Hematoxylin and eosin stain; bar, 90 μm.

neuropil, with or without associated petechial hemorrhages and occasional macrophages. Ischemic damage and necrosis were also evident at this stage, with the appearance of neuronal karyorrhexis and pyknosis of the nuclei of oligodendrocytes and astrocytes. Macrophages were occasionally found throughout involved areas. The most severe lesions (Fig. 5) showed extensive areas of edema, hemorrhage, and infarction, sometimes involving the entire grey matter of the anterior horn (Fig. 5, inset) with destruction of anterior horn cells, neuroglial cells, and other components. Related to these lesions were occlusive fibrin thrombi in capillaries in the affected areas (Fig. 5 and 6). Pyknotic vascular endothelial cell nuclei were seen in both patent and thrombosed vessels. Specific fibrin stains confirmed the presence of fibrin thrombi in the affected vessels and demonstrated marked deposition of fibrin in vascular walls. The mean scores of pathologic changes in the spinal cord (edema, hemorrhage, thrombosis, infarction) were significantly elevated in VT-treated rabbits relative to those in controls ($P < 0.01$) (Fig. 2b). The severity of the CNS histopathology, like that of the cecal pathology, did not correlate directly with the dose of VT1.

Identical pathologic lesions were found in the anterior brain, midbrain, cerebellum, and medulla, although they were less common, less severe, and more focal. The extent of involvement appeared to increase from the anterior to the posterior brain, with the achievement of statistical significance between test and control rabbits only in the analysis of the posterior brain sections (Fig. 2b).

Rabbits exhibiting infection with *Encephalitozoon cuniculi* had findings of vasculitis, perivascular cuffing, focal cerebritis, granulomata, microglial nodules, and leptomeningitis in the brain and spinal cord (29). The findings of VT-related disease were in no way similar to those of encephalitozoan infection. The data from these animals were not included in our findings.

(iii) Other organs. The kidneys were examined in 12 test rabbits and 3 controls. They appeared normal macroscopically, without surface petechial hemorrhages. The glomeruli were of normal size and cellularity, and there was no

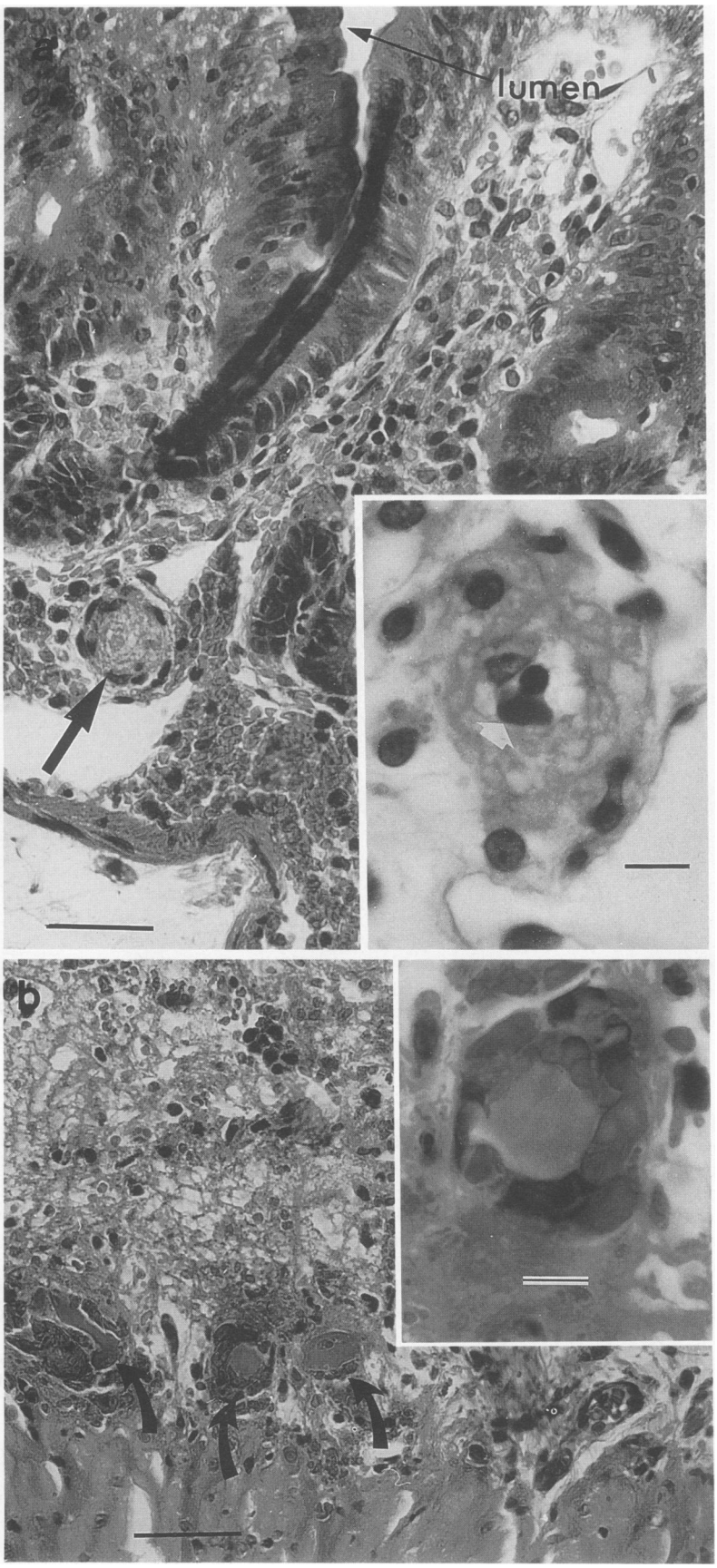
lumen
b

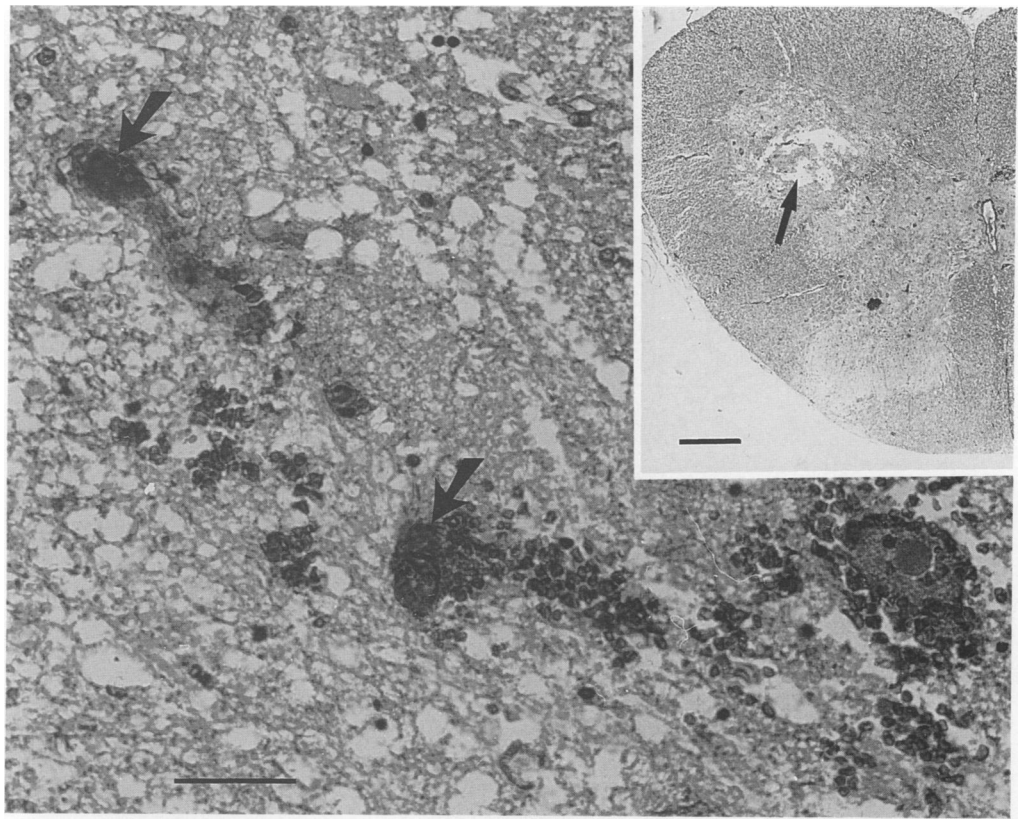

FIG. 5. Widespread hemorrhage, infarction, and edema in the cervical spinal cord of a VT1-intoxicated rabbit. Fibrin thrombi in capillaries are present (arrows). Hematoxylin and eosin stain; bar, 42 μm. The inset shows a low-power view of a large area of infarction (arrow) of the anterior horn of the cervical spinal cord in the same rabbit. Hematoxylin and eosin stain; bar, 890 μm.

evidence of capillary thrombosis or endothelial cell damage. In 2 of 12 test rabbits and in 2 of 3 controls, polymorphonuclear leucocytes were seen in the glomeruli.

Sections from the liver, spleen, pancreas, peritoneal wall, lungs, and heart were taken from five test animals and one control. No microangiopathy or other abnormalities were detected in any of these tissues.

Serum half-life of ^{125}I-VT1. The labelled toxin was eliminated rapidly from the blood after intravenous challenge in the immunologically naive and immune rabbits (Fig. 7), with mean serum half-lives of 1.6 and 2 min, respectively. By 2 h postchallenge, only 3% (naive rabbits) and 6% (immune rabbits) of the ^{125}I-VT1 remained in the blood. In contrast, the ^{125}I-labelled BSA, chosen because it is biologically relatively inert and because its molecular weight is approximately the same as that of VT1, showed a much slower decay from the blood, not even approaching its half-life at 2 h postchallenge. There was no significant difference between the curves for the immune and nonimmune rabbits, although both were significantly different from the curve for BSA (data not shown). Separation of the blood of nonimmune rabbits into serum and erythrocytes revealed that only about 1% of the administered VT was associated with the erythrocyte fraction and that the majority was present in the serum.

Distribution of VT in the rabbit after intravenous challenge. The mean percentages of total administered radioactive VT1 recovered from naive (57%) and immune (46%) rabbits were similar. These measurements were composed of the radioactivity present in all the organs, GI tract (excluding contents), urine, and blood. The remaining 43 to 54% of initial counts is postulated to be retained mainly by the carcass (skin, subcutaneous tissue, skeletal muscle, and skeleton), which was not directly measurable or was not recovered because of quenching or dilution in the tissues.

VT1 localization in the immunologically naive rabbits was highly organ specific (Fig. 8a), with maximal accumulation (counts per minute per milligram per VT dose [counts per minute]) present in the cecum and brain, followed by the small intestine, colon, and spinal cord. All other organs showed comparatively low concentrations of ^{125}I-VT1. The data were also expressed in counts per minute per milligram per unit of flow (milliliters per minute per 100 g) per VT dose

FIG. 4. Cecal vascular pathology in VT1-treated rabbits. (a) Abnormal blood vessel (arrow) in the cecal mucosa. The vascular lumen is occluded by a finely reticular deposit, and the vessel wall is poorly defined. Hematoxylin and eosin stain; bar, 42 μm. The inset shows a high-power view of the thickened, abnormal vascular wall of a submucosal arteriole, with an erythrocyte centrally passing through the narrowed lumen (white arrow). Hematoxylin and eosin stain; oil immersion; bar, 9 μm. (b) Fibrinoid necrosis of the cecal submucosal vessels bordering the muscularis externa (arrows). Hematoxylin and eosin stain; bar, 42 μm. The inset shows a high-power view of amorphous fibrinlike material occluding the lumen of the involved vessel. Hematoxylin and eosin stain; oil immersion; bar, 9 μm.

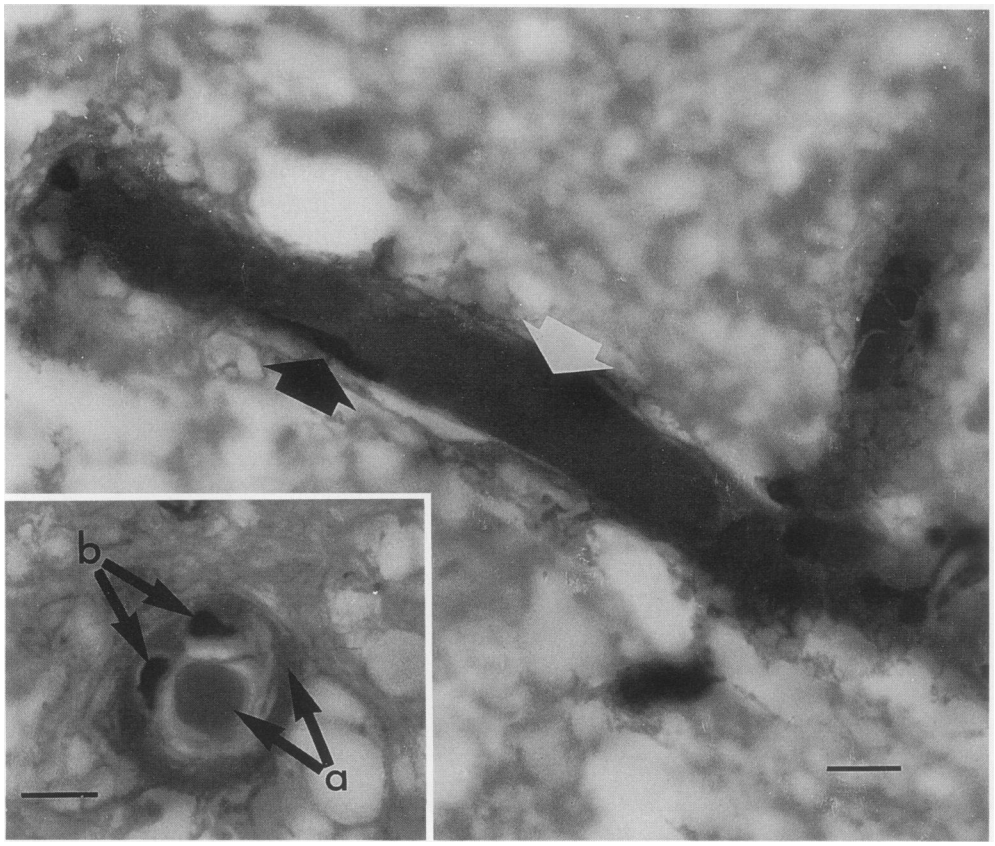

FIG. 6. Thrombosed vessel in the grey matter of the lumbar spinal cord of a rabbit with severe VT-related CNS pathology. This longitudinal section shows occlusion of the vascular lumen by fibrinlike material (white arrow) and pyknotic endothelial cell nuclei (black arrow) lining the vessel lumen. Hematoxylin and eosin stain; oil immersion; bar, 9 μm. The inset shows a cross section of a similarly thrombosed vessel from the cervical spinal cord with fibrin deposition in the lumen and vascular wall (a) and dense, contracted endothelial cell nuclei (b). Hematoxylin and eosin stain; oil immersion; bar, 9 μm.

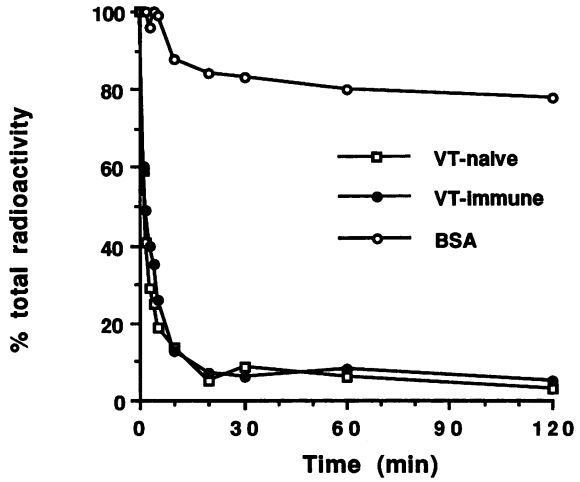

FIG. 7. Serum half-life of ^{125}I-VT1 in nonimmunized (n = 11) and immunized (n = 4) rabbits and serum half-life of ^{125}I-BSA in an immunologically naive rabbit (n = 1). Means of serial measurements are plotted. Error bars not shown. Curves for the half-life of ^{125}I-VT1 are significantly different from that for ^{125}I-BSA ($P < 0.01$) (statistical data not shown).

(counts per minute) to correct for differences in organ blood flow that would affect relative organ distribution (Fig. 8b). Organ blood flow in the rabbit has been well established in studies based on the distribution of intravenously administered radioactively labelled microspheres (20, 30). When the counts per milligram of tissue were corrected for blood flow, the spinal cord now demonstrated the highest accumulation of ^{125}I-VT1, followed by the brain, cecum, colon, and small intestine.

In contrast, the distribution of ^{125}I-VT1 in the immune rabbits showed a markedly different pattern (Fig. 8). The highest specific activity was present in the liver, spleen, and lung, with negligible amounts detected in the GI tract and CNS. The differences between the means of the uptake of radioactivity per gram of tissue in nonimmune and immune rabbits were statistically significant ($P < 0.01$) for all tissues except the kidney, lung, heart, and skeletal muscle (Fig. 8a). Thus, the values for all GI and CNS tissues in naive rabbits were statistically elevated above those of immune rabbits, whereas the values for the spleen and liver in immune rabbits were significantly elevated above those of naive animals. When blood flow is taken into consideration (Fig. 8b), the same statistically significant differences ($P < 0.01$) in ^{125}I-VT1 uptake between naive and immune animals are demonstrated. The clinical and pathologic features of VT intoxication in this experiment could not be assessed because the

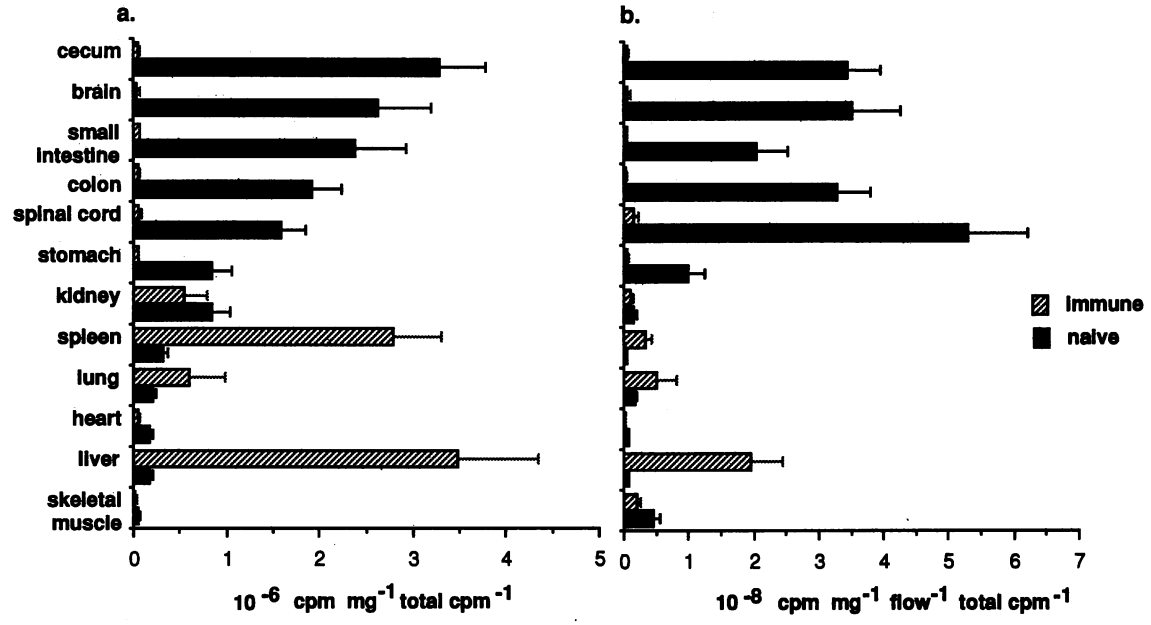

FIG. 8. Localization of ^{125}I-VT1 in tissues of nonimmunized (n = 10) and immunized (n = 4) rabbits. (a) CNS and GI uptake of ^{125}I-VT1 expressed as the mean of the total radioactivity administered. $P < 0.01$ for all values of immunologically naive versus immune animals except for data from kidney, lung, heart, and skeletal muscle tissues. (b) To eliminate the effect of variability in blood flow to different organs, the data include a measure of the flow (milliliters per minute per 100 g of body weight). This has the effect of enhancing the spinal cord uptake in relation to that of other tissues. $P < 0.01$ for all values of immunologically naive versus immune animals except for data from kidney, lung, heart, and skeletal muscle tissues. Error bars represent standard errors of the means.

animals were sacrificed (at 2 h) before these features became evident (18 h at the earliest).

Time course study. The persistence of VT in specific tissues after intravenous injection of ^{125}I-VT1 in eight rabbits was examined (Fig. 9). Two animals were studied at each time (0.03, 2, 9 and 24 hours). The accumulation of VT in the CNS and GI tract was significantly higher than that in all other organs immediately after injection. The rapid accumulation of VT was most prominent in the CNS and increased over the next 9 h, dropping to a level of less than half its peak by 24 h. The specific activity in the CNS was higher than that in the gut at all times except at 24 h. The highly specific binding of VT to CNS and GI tissues was stable over 24 h.

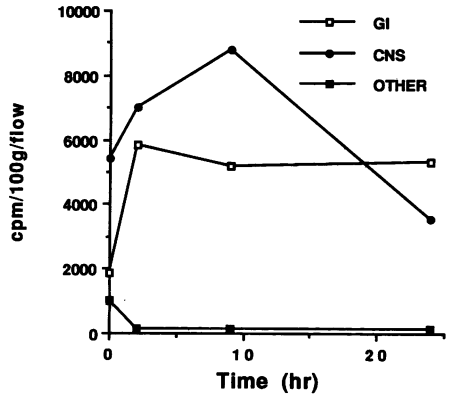

FIG. 9. Distribution of ^{125}I-VT1 in rabbit tissues over time. Radioactivity per 100 g divided by tissue blood flow (milliliters per minute per 100 g of body weight) was determined at 0.03, 2, 9, and 24 h (n = 2 rabbits at each time). Each value is the mean of two measurements; standard errors not shown.

Immunofluorescent localization of VT. Specific and intense fluorescence was detected in both spinal cord and cecal sections from the rabbit given intravenous VT1; this fluorescence was absent in the control. In the cecum, the fluorescence was localized to small and medium-sized vessels in the mucosa and submucosa (Fig. 10). Only certain vessels in a given section showed positive fluorescence. The pattern of the fluorescence appeared to clearly outline the contours of the endothelial cells lining the blood vessel lumen and not to involve any other element. Compared with the cecum, the spinal cord showed a greater percentage of positively stained blood vessels, which were also smaller in caliber (Fig. 11). Fluorescent endothelial cell casts of blood vessels were readily seen throughout the grey matter.

DISCUSSION

Experimental verocytotoxemia in rabbits was found to be an excellent model for exploring the pathogenesis of VT-related disease because of its consistent, reproducible pattern of involvement. The clinical illness was dominated by GI and neurologic involvement and frequently culminated in death. Watery diarrhea, dehydration, anorexia, weight loss, oliguria, and limb paralysis were the cardinal signs of illness. Pathologically, the GI findings were limited to the cecum, which appeared grossly edematous with petechial hemorrhages sprinkled over the mucosa and serosa. The light microscopic features of hemorrhage and edema were associated with thrombotic microvascular angiopathy of the small penetrating vessels of the mucosa and submucosa in the absence of acute or chronic inflammation. These results are consistent with those of Fontaine et al. in their studies

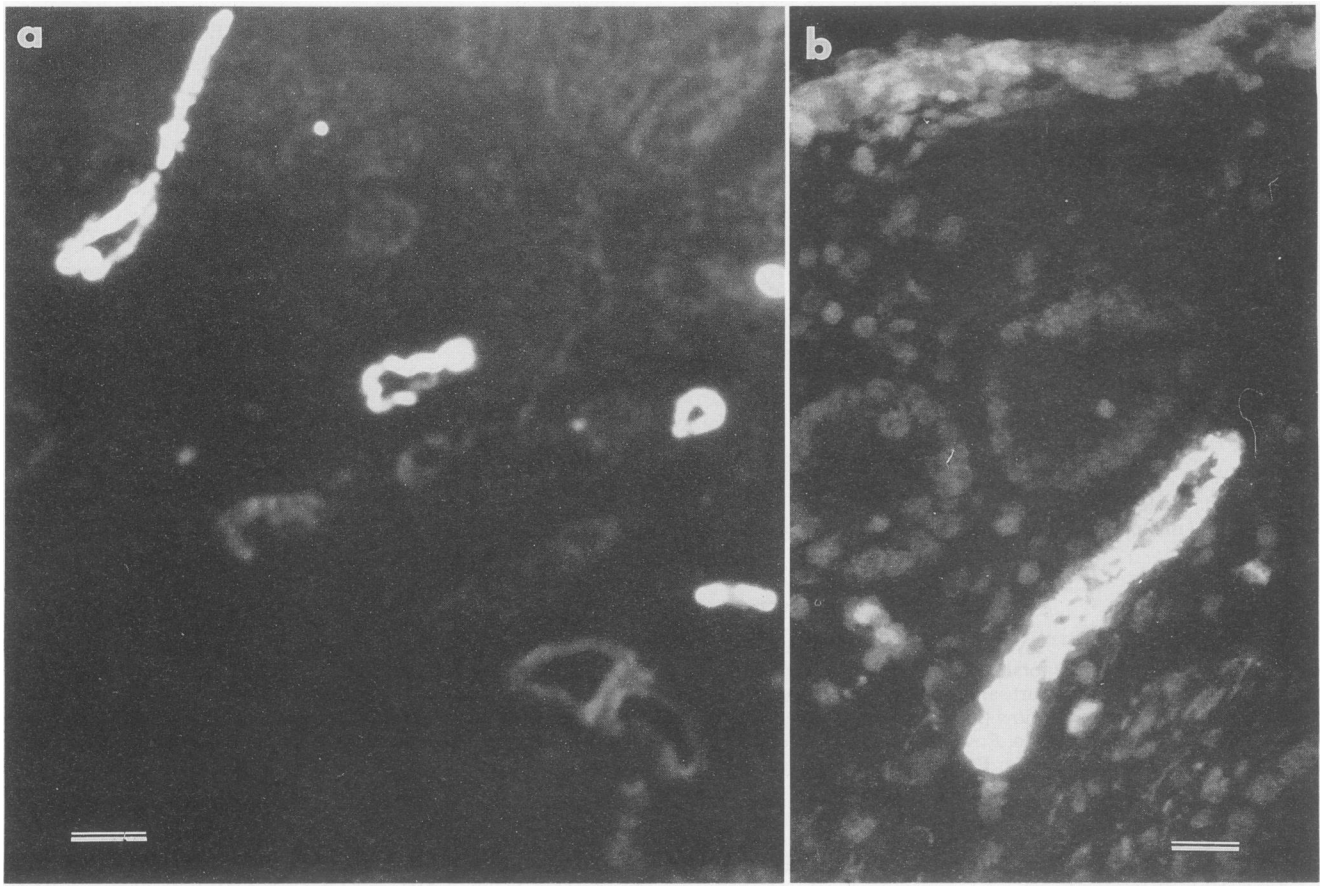

FIG. 10. Immunofluorescent localization of intravenous VT1 in rabbit cecum: fluorescent detection of VT1 in endothelial cells of the submucosal vasculature (a; bar, 90 μm) and in a mucosal feeding vessel (b; bar, 32 μm). A control rabbit cecum showed no fluorescence.

with toxin-negative mutants of *S. dysenteriae* I in the rabbit ileal loop assay and in intragastric challenge experiments with macaque monkeys (7). They observed that the presence of the toxin correlated with the histologic features of epithelial cell layer hemorrhage in the ileal loops of the rabbits and of hemorrhages and destruction of the capillary loops in the interglandular chorion of the colon of the monkey, features which closely resemble the vasculopathy after intravenous VT1 in rabbits.

In our studies, microvascular thrombosis, edema, and hemorrhage were found in the cervical and lumbar expansions of the rabbit spinal cord, areas contributing to the nerve roots forming the brachial and lumbosacral plexuses. Local ischemic necrosis of nerve cells and supporting neural tissue in the grey matter of the cord produced disruption of the nerve supply to the limbs, consistent with the observed paralysis. A direct relationship was noted between VT dose and symptoms of illness, but this relationship did not hold for the comparison of dose and severity of histopathology. This discrepancy may reflect individual variation in response to VT and the large number of animals that would be required to show statistical significance, given this variability. Alternatively, the extent of involvement may not be directly dose related; the initial deleterious effect of VT may set in motion a cascade of host-driven events that then determine the ultimate outcome.

The histopathology of the brain was similar but less pronounced than that observed in the spinal cord. The lesions were most prominent in the cerebellum and posterior brain ($P < 0.05$ compared with controls). Although the anterior and middle brain sections had identical lesions, the small numbers of animals analyzed probably contributed to the lack of statistical significance. There was no significant histopathology in other tissues, including the kidneys. Measurements of renal function showed only transient oliguria and mild elevations of serum creatinine, urea, sodium, and chloride. These abnormalities may have been the result of dehydration related to impaired thirst or an inability to drink in severely paralyzed animals. Significant proteinuria paralleled the toxemia as the only other marker of renal dysfunction. The blood films of the affected rabbits showed no evidence of microangiopathic hemolytic anemia or thrombocytopenia, supporting the observation that renal and hematologic abnormalities are not important manifestations of VT intoxication in rabbits.

The clinicopathologic findings in rabbits support the hypothesis that intravenous VT produces a primary vascular insult and are in agreement with and extend the earlier work of other investigators (3, 5, 12). The predicted physiological result of the vascular damage would be to produce a leaky capillary type of syndrome, resulting in loss of functional integrity of the vessel wall, edema, and hemorrhage, even in the absence of thrombosis. Our findings in the CNS and GI tract support this prediction.

Studies of the localization of ^{125}I-VT1 in tissue demonstrated the rapid disappearance of VT from the blood and its

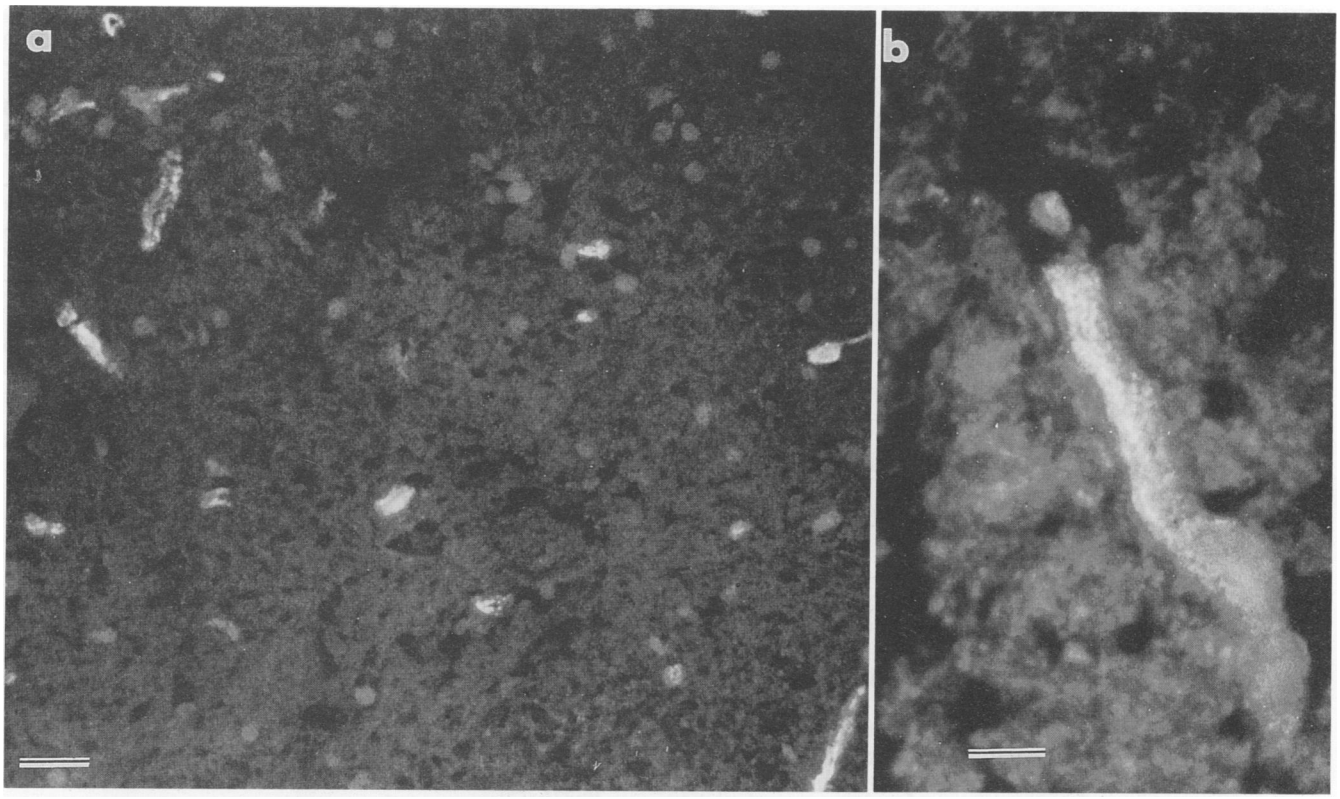

FIG. 11. Immunofluorescent localization of intravenous VT1 in rabbit spinal cord. Fluorescence is limited to endothelial cells of capillaries in the spinal cord (a; bar, 32 μm). (b) High-power view of vascular fluorescence (oil immersion; bar, 9 μm). Spinal cord sections of a control rabbit showed no fluorescence.

specific and stable concentration in CNS and GI tissues. The cecum, brain, small intestine, colon, and spinal cord showed the highest accumulation of the toxin per gram of tissue in immunologically naive rabbits. To take into account the considerable variability in blood flow per unit weight of different organs, the specific tissue accumulation was calculated after correcting for blood flow differences. In descending order, the spinal cord, brain, and cecum now showed the highest specific accumulation of labelled toxin (Fig. 8). These findings correlate closely with the clinicopathologic picture of verocytotoxemia and strongly suggest that the targeting of these tissues is related to highly specific toxin uptake. Furthermore, in immune rabbits, the high uptake in the CNS and GI was totally inhibited, whereas uptake in the liver, spleen, and lung became prominent, probably reflecting the known role of these organs in clearing immune complexes. Immunized rabbits developed neutralizing antibodies to VT1; these antibodies are presumed to be directed against the binding epitope of the B subunit of the toxin (32) and to protect against the biological effects of the toxin. These studies provide further evidence that the targeting of specific rabbit tissues by VT1 is due to their affinity to the toxin, probably facilitated by the presence of specific receptors in those tissues.

Additional investigations that support the above concept come from studies of Lingwood et al. that demonstrate that the glycolipid globotriosyl ceramide (Gb3) is the functional binding receptor for VT1 (18). Gb3 is a major component of the glycolipids in human renal tissue (2) but is absent in the rabbit kidney (36). These and other studies have shown that Gb3 is also present in rabbit and human (11) intestinal tracts and in rabbit brain, all of which are sites of involvement in naturally occurring or experimentally induced VT-related illness. In the rabbit, Gb3 can also be found in the lung and spinal cord but is absent in the heart, liver, and kidney (36). However, the Gb3 was assayed in total tissue extracts and not in the capillary endothelium, which may be the determining site.

The clear parallel between the tissue distribution of the receptor and the clinical, pathologic, and localization data strongly supports the importance of the receptor in the site specificity of VT action. It also provides an explanation for the difference in the spectrum of tissues involved in human HUS and rabbit verocytotoxemia, illnesses which share a histologic common denominator, thrombotic microvascular angiopathy (26). Unexplained at present is the lack of histologic abnormalities in the small intestine and colon of the rabbit tissues that contain Gb3 and concentrated significant quantities of VT1 in our ^{125}I-VT1 localization studies. It may be that VT causes functional abnormalities in these tissues without a visible pathologic correlate or that the VT1-Gb3 binding does not lead to internalization and in vivo action in endothelial cells of these tissues.

Limited immunohistochemical studies showed that VT1 was localized to the endothelial cells of capillaries in the spinal cord and to those of small vessels in the mucosa and submucosa in the cecum. This suggests strongly that VT1 binding to endothelial cells is the initial insult in a pattern of events that leads to clinical illness in rabbits.

Although systemic toxemia after oral challenge with

VTEC in rabbits has not been described, evidence for its occurrence in the gnotobiotic pig model is increasing. Oral challenge with VTEC strains in these animals results in neurologic signs and diarrhea (19, 34). Focal necrosis, hemorrhage, and arteriolar necrosis are seen in the brains of affected animals (8, 34), and toxin activity has been demonstrated in the serum (34). Comparable pathologic lesions were shown in the brain of a child with fatal HUS and neurologic involvement and in the brains of gnotobiotic piglets given the same strain of *E. coli* O157:H7 orally (33). The neuropathology in the pig model correlates closely with that in the rabbit model and also with the infrequently documented vasculopathy in the brain in human HUS (9, 35).

Although systemic toxemia is the postulated pathogenetic mechanism in the widespread lesions of HUS (14), it has not been demonstrated in humans to date. Verocytotoxemia would be expected to occur during the early, intestinal phase of the illness before the presentation and diagnosis of HUS, when high concentrations of free VT have been shown to be present in the stool (15). In addition, its probable short serum half-life (if analogous to that in rabbits) would result in rapid clearance and prevent accumulation in the blood. However, the similarity of the histopathologic lesions in HUS and experimental verocytotoxemia is consistent with a common process (i.e., toxemia) with a variable tissue effect depending on receptor distribution.

Our studies support the hypothesis that VT is of direct pathogenetic significance in HUS and hemorrhagic colitis and that endothelial cells are the primary site of action of the toxin.

ACKNOWLEDGMENTS

This work was supported by grant PG 11123 from the Medical Research Council of Canada. S. E. Richardson was supported by Fellowship 01782 from the Health Research Personnel Development Program of the Ministry of Health of Ontario and by a Fellowship from the Medical Research Council of Canada.

We thank Mary Nahius, Monica Winkler, and Mike Starr for assistance and G. Kent for helpful advice. We also thank C. Lingwood for supplying the monoclonal antibody PH1, J. Brunton for the recombinant strain *E. coli* JB28, and J Konowalchuk for *E. coli* H30.

REFERENCES

1. **Boulanger, J., M. Petric, C. Lingwood, H. Law, M. Roscoe, and M. Karmali.** 1990. Neutralization receptor-based immunoassay for detection of neutralizing antibodies to *Escherichia coli* verocytotoxin 1. J. Clin. Microbiol. **28**:2830–2833.
2. **Boyd, B., and C. Lingwood.** 1989. Verotoxin receptor glycolipid in human renal tissue. Nephron **51**:207–210.
3. **Bridgwater, F. A. J., R. S. Morgan, K. E. K. Rowson, and G. P. Wright.** 1955. The neurotoxin of *Shigella shigae*. Morphological and functional lesions produced in the central nervous system of rabbits. Br. J. Exp. Pathol. **36**:447–453.
4. **Brown, J. E., D. E. Griffin, S. W. Rothman, and B. P. Doctor.** 1982. Purification and biological characterization of Shiga toxin from *Shigella dysenteriae* 1. Infect. Immun. **36**:996–1005.
5. **Cavanagh, J. B., J. G. Howard, and J. L. Whitby.** 1956. The neurotoxin of *Shigella shigae*: a comparative study of the effects produced in various laboratory animals. Br. J. Exp. Med. **37**:272–278.
6. **Fong, J. S. C., J. P. de Chadarevian, and B. Kaplan.** 1984. Hemolytic uremic syndrome. Current concepts and management. Pediatr. Clin. N. Am. **29**:835–856.
7. **Fontaine, A., A. Josette, and P. J. Sansonetti.** 1988. Role of Shiga toxin in the pathogenesis of bacillary dysentery, studied by using a *tox* mutant of *Shigella dysenteriae* 1. Infect. Immun. **56**:3088–3109.
8. **Francis, D. H., R. A. Moxley, and C. Y. Androas.** 1989. Edema disease-like brain lesions in gnotobiotic piglets infected with *Escherichia coli* serotype O157:H7. Infect. Immun. **57**:1339–1342.
9. **Gianantonio, C., M. Vitacco, F. Mendilaharzu, G. E. Gallo, and E. T. Sojo.** 1973. The hemolytic uremic syndrome. Nephron **11**:174–192.
10. **Hii, J. H., C. Gyles, T. Morooka, M. A. Karmali, R. Clarke, S. de Grandis, and J. L. Brunton.** 1991. Development of verotoxin 2 and verotoxin 2 variant (VT2v)-specific oligonucleotide probes on the basis of the nucleotide sequence of the B cistron of VT2v from *Escherichia coli* E32511 and B2F1. J. Clin. Microbiol. **29**:2704–2709.
11. **Holgersson, J., N. Strömberg, and M. E. Breimer.** 1988. Glycolipids of human large intestine: difference in glycolipid expression related to anatomical localization, epithelial/non-epithelial tissue and the ABO, *Le* and *Se* phenotypes of the donors. Biochimie **70**:1565–1574.
12. **Howard, J. G.** 1955. Observations on the intoxication produced in mice and rabbits by the neurotoxin of *Shigella shigae*. Br. J. Exp. Pathol. **36**:439–446.
13. **Huang, A., S. de Grandis, J. Friesen, M. Karmali, M. Petric, R. Congi, and J. L. Brunton.** 1986. Cloning and expression of the genes specifying Shiga-like toxin production in *Escherichia coli* H19. J. Bacteriol. **166**:375–379.
14. **Karmali, M. A.** 1989. Infection by verocytotoxin-producing *Escherichia coli*. Clin. Microbiol. Rev. **2**:15–38.
15. **Karmali, M. A., M. Petric, C. Lim, R. Cheung, G. S. Arbus, and H. Lior.** 1985. The association between idiopathic hemolytic uremic syndrome and infection by verotoxin-producing *Escherichia coli*. J. Infect. Dis. **151**:775–782.
16. **Konowalchuk, J., J. I. Speirs, and S. Stavric.** 1977. Vero response to a cytotoxin of *Escherichia coli*. Infect. Immun. **18**:775–779.
17. **Kozma, C., W. Macklin, L. M. Cummins, and R. Mauer.** 1974. The anatomy, physiology, and the biochemistry of the rabbit, p. 50–72. *In* S. H. Weisbroth, R. E. Flatt, and A. L. Kraus (ed.), The biology of the laboratory rabbit. Academic Press, Inc., New York.
18. **Lingwood, C. A., H. Law, S. E. Richardson, M. Petric, J. L. Brunton, S. de Grandis, and M. A. Karmali.** 1987. Glycolipid binding of purified and recombinant *Escherichia coli* produced verotoxin in vitro. J. Biol. Chem. **262**:8834–8839.
19. **Moxley, R. A., D. H. Francis, H. Karch, and E. D. Erickson.** 1987. Comparative pathogenesis of infections with bovine and human origin enterohemorrhagic *Escherichia coli* (EHEC) in gnotobiotic piglets. International Symposium and Workshop on Verocytotoxin-producing *Escherichia coli* Infections, Toronto, Canada., abstr. AMV-3.
20. **Neutze, J. M., F. Wyler, and A. M. Rudolph.** 1968. Use of radioactive microspheres to assess distribution of cardiac output in rabbits. Am. J. Physiol. **215**:486–495.
21. **O'Brien, A. D., and R. K. Holmes.** 1987. Shiga and Shiga-like toxins. Microbiol. Rev. **51**:206–220.
22. **Obrig, T. G., P. J. Del Vecchio, J. E. Brown, T. P. Moran, B. M. Rowland, T. K. Judge, and S. W. Rothman.** 1988. Direct cytotoxic action of Shiga toxin on human vascular endothelial cells. Infect. Immun. **56**:2373–2378.
23. **Pai, C. H., J. K. Kelly, and G. L. Meyers.** 1986. Experimental infection of infant rabbits with verotoxin-producing *Escherichia coli*. Infect. Immun. **51**:16–23.
24. **Petric, M., M. A. Karmali, S. Richardson, and R. Cheung.** 1987. Purification and biological properties of *Escherichia coli* verocytotoxin. FEMS Microbiol. Lett. **41**:63–68.
25. **Reed, L. J., and H. Muench.** 1938. A simple method of estimating fifty percent endpoints. Am. J. Hyg. **27**:493–497.
26. **Richardson, S. E., M. A. Karmali, L. E. Becker, and C. R. Smith.** 1988. The histopathology of the hemolytic uremic syndrome (HUS) associated with verocytotoxin-producing *Escherichia coli* (VTEC) infections. Hum. Pathol. **19**:1102–1108.

26a. **Sandvig, K., S. Olsnes, J. E. Brown, O. W. Petersen, and B. van Deurs.** 1989. Endocytosis from coated pits of Shiga toxin: a glycolipid-binding protein from Shigella dysenteriae 1. J. Cell

Biol. **108**:1331–1343.
27. **Schägger, H., and G. von Jagow.** 1987. Tricine-sodium dodecyl sulfate-polyacrylamide gel electrophoresis for the separation of proteins in the range from 1 to 100 kDa. Anal. Biochem. **166**:368–379.
28. **Schmitt, C. K., M. L. McKee, and A. D. O'Brien.** 1991. Two copies of Shiga-like toxin II-related genes common in enterohemorrhagic *Escherichia coli* strains are responsible for the antigenic heterogeneity of the O157:H7 strain E32511. Infect. Immun. **59**:1065–1073.
29. **Shadduck, J. A., and S. P. Pakes.** 1971. Encephalitozoonosis (nosematosis) and toxoplasmosis. Am. J. Pathol. **64**:657–674.
30. **Smith, D. R., H. J. Smith, and R. K. Rajjoub.** 1978. Measurement of spinal cord blood flow by the microsphere technique. Neurosurgery **2**:27–30.
31. **Strockbine, N. A., M. P. Jackson, L. M. Sung, R. K. Holmes, and A. D. O'Brien.** 1988. Cloning and sequencing of the genes for Shiga toxin from *Shigella dysenteriae* type 1. J. Bacteriol. **170**:1116–1122.
32. **Strockbine, N. A., L. R. M. Marques, R. K. Holmes, and A. D. O'Brien.** 1985. Characterization of monoclonal antibodies against Shiga-like toxin from *Escherichia coli*. Infect. Immun. **50**:695–700.
33. **Tzipori, S., C. W. Chow, and H. R. Powell.** 1988. Cerebral involvement with *Escherichia coli* O157:H7 in humans and gnotobiotic piglets. J. Clin. Pathol. **41**:1099–1103.
34. **Tzipori, S., K. I. Wachsmuth, X. Smithers, and C. Jackson.** 1988. Studies in gnotobiotic piglets on non-O157:H7 *Escherichia coli* serotypes isolated from patients with hemorrhagic colitis. Gastroenterology **94**:590–597.
35. **Upadhyaya, K., K. Barwick, M. Fishaut, M. Kashgarian, and N. J. Siegel.** 1980. The importance of nonrenal involvement in hemolytic-uremic syndrome. Pediatrics **61**:115–120.
36. **Zoja, C., D. Corna, C. Farina, G. Sacchi, C. Lingwood, M. Doyle, V. V. Padhye, M. Abbate, and G. Remuzzi.** Tissue localization of verotoxin glycolipid receptor determines clinical expression of the disease in rabbits challenged with verotoxin-1. J. Lab. Clin. Med., in press.